Weighted Quasi-Newton and Variable-Order, Variable-Step Adams Algorithm for Determining Site-Specific Reaction Rate Constants

Fei He and Alan G. Marshall*,†

National High Magnetic Field Laboratory, Florida State University, 1800 East Paul Dirac Dr., Tallahassee, Florida 32310

Received: August 12, 1999; In Final Form: October 29, 1999

A weighted quasi-Newton algorithm for function minimization and a variable-order, variable-step Adams algorithm for ordinary differential equations were combined to solve site-specific gas-phase reaction rate constants. If the systems appear to be "stiff", smaller steps were taken in Adams method to search for the solution. A user supplied error tolerance was used to determine the accuracy of the solution. Upon the return of each solution, a weighted algorithm is introduced into the calculation of X^2 to minimize interference from noise. Lower and upper bounds for reagent fraction and rate constants were applied to ensure the validity of the results. The search direction is calculated by a quasi-Newton algorithm. When a saddle point is suspected, a local search is carried out with a view to moving away from the saddle point. The information obtained from site-specific rate constants may provide further insight into the reaction mechanism as well as gas-phase structure. It can be applied to gas-phase H/D exchange, deprotonation, and other reactions.

I. Introduction

A. Need for Site-Specific Rate Constants. Extraction of individual chemical reaction rate constants from the time dependence of the observed concentrations of reactants and products for a sequence of reactions is straightforward, provided that each reaction step produces chemically inequivalent products

$$A \xrightarrow{k_a} B \xrightarrow{k_b} C \quad \text{(no restriction on } k_a/k_b) \tag{1}$$

as shown in Figure 1 (top). A similar analysis is approximately correct for reactions with multiple chemically indistinguishable products (say, successive ligand substitutions at a single atom or replacement of hydrogen by deuterium at different sites on the same reagent molecule) formed with very different rate constants:

$$D0 \xrightarrow{k_a} D1 \xrightarrow{k_b} D2 \; k_a \gg k_b \tag{2}$$

in which D0, D1, and D2 denote molecules containing a total of zero, one, or two deuteriums in place of hydrogens, as shown in Figure 1 (bottom).

However, kinetic analysis becomes fundamentally different for reactions with multiple chemically indistinguishable products with similar (i.e., to within 1−2 orders of magnitude) formation rate constants. For example, consider an H/D exchange mechanism, for two exchangeable hydrogens of similar deuterium replacement rate constant.

$$A(H_aH_b) \xrightarrow{k_1} A(H_aD_b) \xrightarrow{k_2} A(D_aD_b) \tag{3a}$$

$$A(H_aH_b) \xrightarrow{k_2} A(D_aH_b) \xrightarrow{k_1} A(D_aD_b) \text{ (No restriction on } k_1/k_2) \tag{3b}$$

We seek the *individual* (site-specific) rate constant, k_1 and k_2. However, if we simply fit the time dependence of the (experimentally observable) $A(H_2)$, $A(HD)$, and $A(D_2)$ concentrations according to eq 2, we obtain *apparent* rate constants, k_a and k_b, that differ from the (true) individual rate constants, k_1 and k_2. The difference is especially obvious (see Figure 2) for two (kinetically) equivalent exchangeable hydrogens, for which the individual deuterium replacement rate constants are in the proportion, ($k_1 = 2k_2$), whereas the apparent rate constants (from eq 2) are different ($k_a \approx 2.5k_b$).

For H/D exchange, for example, the deuterating reagent (e.g., D_2O) is usually in great excess so that each step of the kinetic model may be described by a pseudo-first-order rate constant: k_1, k_2, k_3, etc. In this paper, we present a general algorithm, and code it in C language (available on request) for a personal computer, to generate site-specific rate constants from an unbranched series of chemical reactions. The method is demonstrated for simulated and experimental H/D exchange reactions of the type encountered in experiments designed to map the solvent accessibility of exchangeable hydrogen sites on solution-phase or gas-phase biomacromolecules (e.g., peptides, proteins, nucleic acids, etc.).

B. H/D Exchange Kinetics. Solution-phase hydrogen/deuterium (H/D) exchange reactions, observed primarily by NMR, provide insight into mechanism and structure of (e.g.) proteins.[1−3] The general finding is that H/D exchange is slower for amide hydrogens involved in hydrogen-bonding (e.g., α-helix, β-sheet) and/or amide hydrogens buried in the interior of the macromolecule[4] or at a contact surface between the protein and its adduct.[5] Although gas-phase H/D exchange for similar purposes has been investigated for decades,[6,7] such experiments have only recently been applied to peptides and nucleotides[8−12] and to the tertiary structure of proteins.[13−18] An advantage of the gas-phase experiment is that *all* exchangeable hydrogens (not just the slowly exchanged amide backbone hydrogens) may be characterized, because the pressure can be set sufficiently low ($<10^{-7}$ Torr) that the rate for replacement of even the first hydrogen can be observed.[19] Gas-phase proton-transfer reaction kinetics has been applied to small organic

* To whom correspondence may be addressed.
† Member of the Department of Chemistry, Florida State University, Tallahassee, FL.

10.1021/jp9928715 CCC: $19.00
Published on Web 12/28/1999

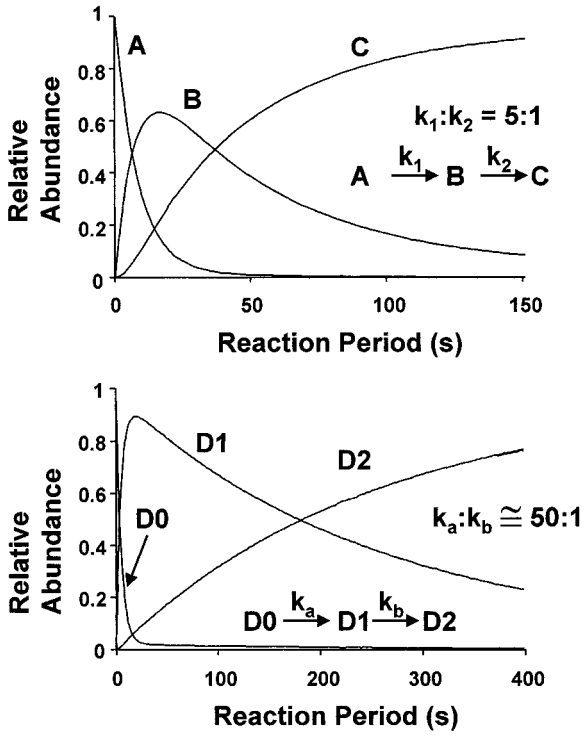

Figure 1. Kinetics analysis of consecutive chemical reactions. Top: concentration vs reaction period for all three species in a system of two consecutive reactions (arbitrary relative rate constants) for which the products formed after each step are chemically distinguishable. Bottom: as above, but for two successive H/D replacement reactions for which the intermediate species can be formed (with widely different rate constants) to form two chemically indistinguishable forms. Because the rate constants are so different, this system can (to a good approximation) be treated like the example above it. D0, D1, and D2 denote species in which a *total* of zero, one, or two hydrogens has been replaced by deuterium.

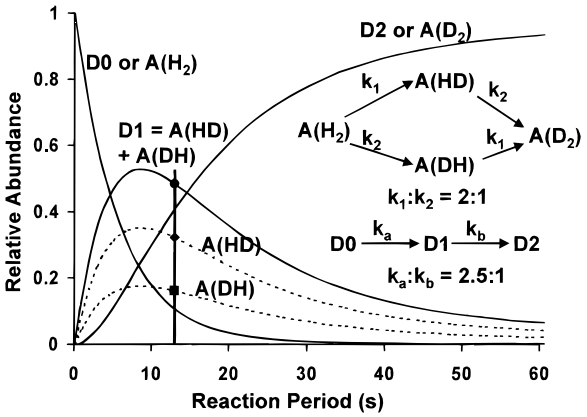

Figure 2. Concentration vs reaction period for all four species, AH_2, AHD, AHD, and AD_2, in a system of two successive H/D replacement reactions (slightly different rate constants) for which the intermediate products formed after one step are chemically indistinguishable. Site-specific kinetic analysis (see below) yields the true individual rate constants, k_1 and k_2. As shown by the filled circles at a particular reaction period, the concentration, [D0], of molecules containing a total of 1 deuterium is the sum of the concentrations of species in which the hydrogen at the first or second site is replaced by deuterium. An attempt to fit this system of reactions by the model of Figure 1 (bottom) yields apparent rate constants, k_a and k_b, which differ significantly from the site-specific rate constants, k_1 and k_2 (see text).

compounds[20,21] and recently larger biomolecules.[22,23] Although most prior kinetics analyses of such systems have extracted only *apparent* rate constants,[24,25] it has been pointed out that site-specific rate constants give more insights into the structure and reaction mechanism.[26,27]

C. Prior Methods for Extracting Rate Constants. Wagner et. al. reported a method to calculate pseudo-first-order rate constants by fitting a reactant concentration vs time profile.[28] However, that method requires that the rate constants differ sufficiently in magnitude such that different segments of the reactant concentration vs time profile can be distinguished visually, thereby limiting applicability and reliability. Zhang et. al. introduced a maximum entropy algorithm[29] designed for solution-phase H/D exchange, for which (unlike the corresponding gas-phase experiment) the fraction of deuterium in the deuterating reagent is known, say 90:10 D_20/H_20. Also, the MEM approach gives a probability distribution of rate constants (i.e., a curve in which each peak area represents the number of hydrogens with rate constants within a specified rate constant range), rather than a direct estimate of each rate constant. Another limitation of the above-mentioned methods is that they utilize only the average deuterium incorporation number and thus do not yield rate constants with high precision.

Gard et. al. published an algorithm for solving differential equations and calculating site-specific rate constants.[27] Although the algorithm works well,[30] it is realized in Mathematica (Wolfram Research, Champaign, IL) and hence cannot be used as a stand-alone executable program. Moreover, that program requires pre-installation of Mathematica and is limited in computation speed because the program is not available as a compiled version.

D. A New Approach. Here, we present an algorithm and computer software to calculate site-specific rate constants, combining a quasi-Newton algorithm for function minimization and a variable-order, variable-step Adams algorithm to solve a set of ordinary differential equations. The system checks for possible "stiffness" (see below) in the equations; if stiffness is identified, then smaller increments are taken in the Adams algorithm. A user-supplied error tolerance determines the accuracy of the differential equation solution. A weighting factor is introduced into the evaluation of X^2 (chi-square) in the quasi-Newton algorithm to minimize the interference by noise. Lower and upper bounds for reagent fraction of deuterium and rate constants are applied to ensure the validity of the results. If a saddle point is suspected, a local search is carried out with a view to moving away from the saddle point. The program displays the fitted and experimental reactant and product concentration vs time profiles as well as mean square error; thus, one can adjust the initial rate constant guesses accordingly to achieve better results. Finally, we provide experimental examples and discuss advantages and disadvantages of the new algorithm.

II. Methods

Although it will be obvious that the present method applies to other kinetics problems (e.g., successive substitution of ligands in a metal complex), we shall describe the problem as H/D exchange with deuterated methanol CH_3OD. Generally, multiple exchanges (for a molecule with n exchangeable hydrogens) are possible and one observes experimentally the disappearance of the reactant parent molecule (represented as zero deuteriums, D_0) and the growth of products with increasing number of incorporated deuteriums (D_1, D_2, D_3, etc.) Rather than treating the system as one of successive exchanges with apparent rate constants k_n for each exchange.[24,25] we treat the system as n independent exchangeable sites, each with its site-specific rate constant, so that exchange at the jth site follows

the simple first-order rate law,

$$H_j + CH_3OD \underset{k_{-j}}{\overset{k_j}{\rightleftharpoons}} D_j + CH_3OH \quad 1 \le j \le n \tag{4}$$

In which H_j and D_j are the unexchanged and exchanged forms of the jth site, with the exchange and back-exchange rate constants, k_j and k_{-j}. The resulting differential equation,

$$\frac{d[D_j]}{dt} = k_j[H_j][CH_3OD] - k_{-j}[D_j][CH_3OH] \tag{5}$$

describes the time dependence of the concentration, $[D_j]$, of deuterium-substituted product at the jth site. Kinetic isotopic effects in gas-phase proton transfer and H/D exchange reactions are negligible.[31] It is thus safe to assume that

$$k_j = k_{-j} \tag{6}$$

so eq 5 simplifies to

$$\frac{d[D_j]}{dt} = k_j[H_j][CH_3OD] - k_j[D_j][CH_3OH] \tag{7}$$

For gas-phase H/D exchange experiments, it is usual to "condition" the vacuum chamber (by prolonged exposure to deuterating agent, in this case, CH_3OD) prior to reaction. Nevertheless, a certain proportion of undeuterated agent (in this case, CH_3OH) will be present, due to back-exchange with species adsorbed to vacuum chamber wall or water molecules from the ionization source (e.g., electrospray ionization). We therefore treat the uncertainty in the fraction of deuterium in the deuterating agent by introducing another (initially unknown) parameter, f_D, so that eq 7 may be rewritten as

$$\frac{d[D_j]}{dt} = k_j[H_j]f_D[CH_3OH(D)] - k_j[D_j][1 - f_D][CH_3OH(D)] \tag{8}$$

in which $[CH_3OH(D)]$ denotes the total pressure of methanol (whether deuterated or not).

Given initial guesses for k_j and f_D, one can solve eq 8 to yield the concentrations (actually, relative abundances) of H_j and D_j at the jth individual site as a function of time during the reaction. For n independent sites, one constructs and solves a set of n such differential equations. At any given time during the reaction, the relative abundance of molecules containing a total of d deuteriums ($0 \le d \le n$), is then obtained by adding up the appropriate concentrations (e.g., {A(HD) + A(DH)} for two sites in Figure 2, {A(HHD) + A(HDH) + A(DHH)} for three sites, etc.). The algorithm thus consists of iteratively varying the initial guesses for k_j and f_D until the calculated and experimentally observed relative abundances of molecules with d deuteriums ($0 \le d \le n$) agree to within a specified difference.

The overall algorithm is shown in Figure 3. Initial values for f_D and n different k_j are set by the program automatically by carrying out trial calculations based on the experimentally measured CH_3OD pressure and the decay of the parent reactant. A variable-order, variable-step Adams algorithm then solves the set of differential equations.[32] The first time point (usually taken as time zero) defines the initial conditions; hence, the program can be applied to reactions started from a isotopic mass distribution (say, natural abundance) or an isolated monoisotopic mass.[11] Although kinetic systems are rarely found to be "stiff", as a precaution, the program checks for "stiffness" (i.e., solutions with rapidly decaying components, thus rendering the solution unstable). If found, the program will use (empirically determined) smaller steps in the Adams algorithm to preserve stability. Several algorithms are available for solving ordinary differential equations, e.g., Adams, backward differentiation formulas (BDF), and Runge−Kutta. In general, the Runge−Kutta method is applied to nonstiff systems. Although both Adams and BDF methods may be applied to stiff systems, we chose the Adams method for its accuracy and efficiency of integration over a long range of data, as in concentration vs time profiles in chemical reaction kinetics.[32]

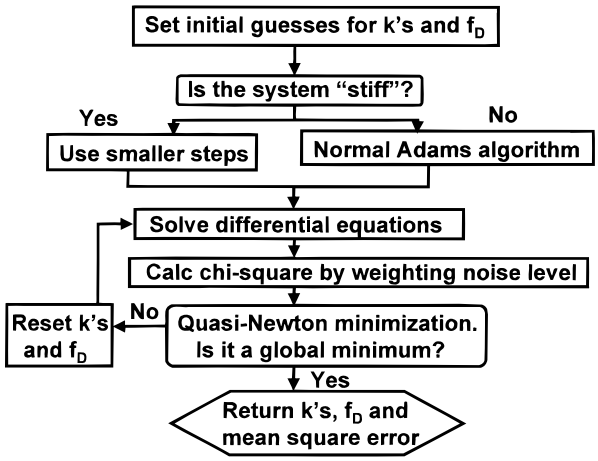

Figure 3. Flowchart for an algorithm to compute site-specific rate constants.

Finally, the user can vary the specified error tolerance (between calculated and experimental relative abundances) to adjust the accuracy and total computation time. The Adams method returns abundances of each deuterated species at the same reaction time values as the experimental data.

A chi-square value, χ^2, of the results may be calculated as

$$\chi^2 = \sum_{i=1}^{M}\sum_{j=0}^{n}(A_{calc}(i,j) - A_{expt}(i,j))^2 \tag{9}$$

in which $A_{calc}(i,j)$ and $A_{expt}(i,j)$ are the calculated and experimental normalized relative abundances of species j (from $j = 0$, i.e., parent species, to $j = n$, the species Dn with all n sites deuterated), and M is the number of time increments in the experimental data (i.e., number of data points taken in the time course of the reaction). However, in the presence of detector-limited white noise,[33] low-abundance species will exhibit a lower signal-to-noise ratio and thus a higher error. We therefore introduce a weight factor, g, $0 < g < 1$, to minimize that effect; $g(i,j)$ is linearly proportional to the relative abundance at each time-course point so that species with higher abundance contribute greater weight in the computation.

$$\chi^2 = \sum_{i=1}^{M}\sum_{j=0}^{n}\{g(i,j)[A_c(i,j) - A_e(i,j)]\}^2 \tag{10}$$

It is also commonly noted in gas-phase kinetic studies that the reaction log(concentration) vs time profile during the initial stages of the reaction plot exhibits curvature because the reactant ions are not yet completely thermalized.[8,27] Because the parent reactant (namely, the undeuterated species) has very high relative initial abundance, we reduce its weight factor initially to reduce error due to incomplete thermalization. Specifically, the user can choose to reduce the weight factor (say, $0.3 < g < 0.5$) for

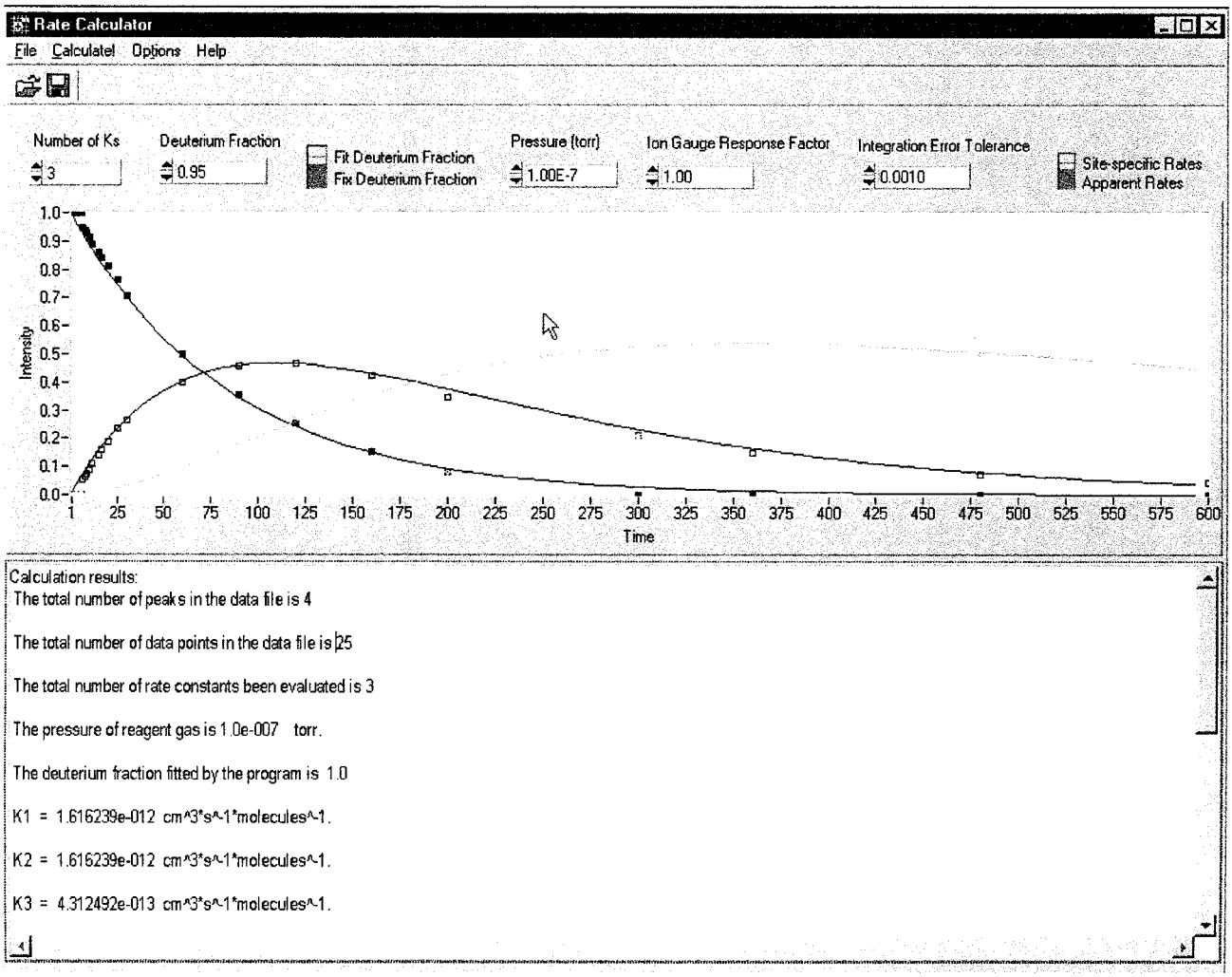

Figure 4. Screen dump showing the user interface for extraction of site-specific rate constants from a series of H/D exchange reactions. The user can access all options and parameters intuitively through menu and interface panel controls. The calculated results are displayed both in a text box and graphically, allowing the user to adjust the initial parameter estimates to achieve the best fit to experimental concentration vs time data.

initial data points (typically 2−5 s) for which the semilog reaction time course plot shows curvature.

The χ^2 value obtained above is then subjected to minimization by the quasi-Newton method[34,35] with respect to f_D and the n different k_j parameters. Validity of the final result is further enhanced by setting upper and lower bounds for k_j (corresponding to between 0.001% and 100% efficiency for a pseudo-first-order reaction) and f_D (0.5−1.0). The user can also specify the value of f_D if it is known for certain experiments (e.g., deprotonation reactions, for which there is no reverse reaction, so that $f_D = 1$). The search direction after each iteration is based on a gradient vector, whose components are the first partial derivatives of χ^2 with respect to each parameter. At each iteration of the search, the differential equations are solved again from the new k_j and f_D values returned by quasi-Newton algorithm until a convergence is found. Upon exit from the calculation, the mean square error is also reported.

Searches for possible local minima or saddle points are built into the quasi-Newton module. If a saddle point is suspected, a local search (with a small perturbation of the fit parameters) is carried out with a view to moving far enough away from the saddle point to find other local minima. The same approach applies to local minima. However, validating a local minimum may be more difficult than locating a saddle point and the algorithm cannot guarantee to discriminate between a local and global minimum. To that end, the user can examine the display of the fitted curves and the mean square error. If a local minimum is suspected, the user can then change the initial guesses for the rate constants and reissue the calculation until the result fails to improve further.

Apparent rate constants can also be calculated by this program. In that case, *N-coupled* (as opposed to *N-independent*) differential equations are constructed,[27] and the same algorithm is applied. The user can access that choice by a simple binary switch.

III. Experimental Section

H/D exchange experiments of amino acids and dipeptides were carried out with a home-built 9.4 T superconducting magnet FT-ICR.[36] All amino acids and dipeptides are purchased from Aldrich Chemical Co. (Milwaukee, WI) except the methyl esters of dipetides which were custom-synthesized by the BASS Laboratory at Florida State University. Each electrospray solution was prepared in 50:50 (v/v) MeOH/H_2O with 2% (v/v) acetic acid and infused into a tapered 50 μm i.d. fused silica micro-ESI needle[37] at a flow rate of 300 nL/min. The needle electric potential was +2000 V relative to the vacuum chamber (ground). Ions were accumulated in a linear octopole for 3−5 s before transfer through a second octopole ion guide to the ICR cell.

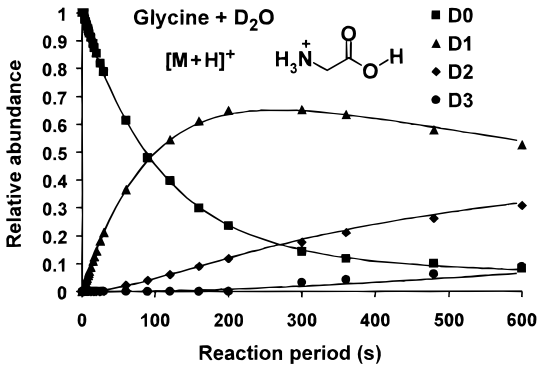

Figure 5. Experimental and best-fit theoretical fit to relative abundances of singly protonated glycine during reaction with D_2O. Monoisotopic protonated molecular glycine ions, $[^{12}C_2{}^1H_5{}^{14}N^{16}O_2 + {}^1H]^+$ isolated by stored waveform inverse Fourier transform (SWIFT) dipolar excitation are exposed to gaseous D_2O (7.4×10^{-8} Torr). The experimental relative abundances of glycine in which zero (■), one (▲), two (◆), and three (●) hydrogens have been replaced by deuteriums are fitted by the solid curve according to the site-specific kinetics method outlined in Figures 2 and 3. (The data for incorporation of four deuteriums was not included in the calculation because of its low abundance (taken into account automatically by the program)).

Prior to each experiment, a static pressure of D_2O was introduced by a precision leak valve and allowed to stabilize for 4 h. Ions trapped in the ICR cell were allowed to cool for 1 s. All species except the monoisotopic peak of the species subject to H/D exchange were ejected by SWIFT[38,39] dipolar excitation. After isolation, ions were allowed to react with background D_2O for each of several exchange periods before detection. Signal-to-noise ratio was enhanced by co-adding 3−5 time-domain data sets. All mass spectra were acquired with an Odyssey data system (ThermoQuest, Bremen, Germany). The co-added time-domain ICR data were subjected to baseline correction followed by Hanning apodization and one zero fill before Fourier transformation and magnitude calculation.

IV. Discussion

The above-described algorithm was programmed in C and compiled in CVI/LabWindows (National Instruments, Austin, Texas). Optimized numerical libraries from Numerical Algorithm Group (Downers Grove, IL) improved computational efficiency. The program interface is shown in Figure 4. Fitted curves are displayed along with experimental data, making it easy to judge the quality of the optimization. The initial parameter guesses may then be varied to achieve the best fit. Because the algorithm executes as a compiled program with optimized libraries, execution speed is fast. For example, the time required for best fit evaluation of all four k_j's for glycine was ∼5 s on a Pentium-based computer.

We have tested the program with both simulated and experimental data, both with excellent results. For simulated data, the best-fit rate constants agree with the true values to within ∼1%. We have also applied the program to singly charged cationic gas-phase amino acids (glycine, sarcosine, glycine methyl ester, and sarcosine methyl ester) and dipeptides (diglycine, GlySar, and their methyl esters) reacting with D_2O. Figure 5 shows the result of fitting replacement of the first three protons of the gas-phase $[\text{glycine} + H]^+$ with deuterium from D_2O. The analysis yields one fast exchange site ($k_1 = 2.85 \times 10^{-12}$ cm^3 s^{-1} molecule^{-1}) and three equivalent slow-exchanging sites, $k_2 = k_3 = k_4 = 1.39 \times 10^{-13}$ cm^3 s^{-1} molecule^{-1}, in good agreement with a prior analysis of the same system.[30] It seems clear that the three equivalent slow exchanging protons are from the amino terminal $-NH_3^+$ site, and that the remaining fast-exchanging hydrogen is the carboxyl −COOH group. We shall report separately on results for other amino acids, dipeptides, and their methyl esters, in experiments designed to identify which exchangeable hydrogen is which (by blocking one of each of various sites by substitution of methyl for hydrogen).

The reader may note that data from the D_4 species for glycine was not included in the calculation due to its very low relative abundance even at maximum reaction period. Nevertheless, because *all* of the deuterated species, such as D_1, D_2, and D_3 contain contributions from *all* four site-specific rate constants, it is possible to determine the four rate constants without including the D_4 data directly in the calculation. This approach is appropriate only for noisy spectra, however, due to its obvious limitations: first, if some deuterated species are missing, then the calculation will not be as reliable; second, if the rate constants differ significantly, then the contribution of the slowest rate for all other species is minimal and the calculated results will exhibit significant errors. Thus, one should ordinarily use data from all available and exchanged species in the calculation.

The present program makes use of the time-dependent relative abundances of *all* observed deuterated species rather than just the parent or average deuterium incorporation, and therefore should prove more accurate and reliable for determining site-specific rate constants. Provision for back-exchange of the deuteration reagent into the calculation should further improve the accuracy of the rate constant determination. The major remaining source of error will likely originate from the difference in pressure at a spatially remote ion gauge and that in the trapped-ion cell, assuming that the ion gauge has been properly calibrated for the deuterating agent of interest.

The site-specific exchange algorithm is necessarily computationally intensive due to its need to solve differential equations iteratively to optimize the rate constant estimates. Moreover, the complexity of searching a multidimensional surface increases exponentially with an increasing number of k's. Thus, the determination of site-specific rate constants becomes increasingly difficult for more than ∼15 exchangeable sites.

Acknowledgment. The authors thank Dr. M. Kirk Green for helpful discussions and Dr. Michael A. Freitas for helpful suggestions. This work was supported by grants from the NSF National High Field FT-ICR Mass Spectrometry Facility (CHE-94-13008), NIH(GM-31683), Florida State University, and the National High Magnetic Field Laboratory in Tallahassee, Florida.

References and Notes

(1) Schmid, F. X.; Baldwin, R. M. *J. Mol. Biol.* **1979**, *135*, 199−215.
(2) Roder, H.; Elove, G. A.; Englander, S. W. *Nature* **1988**, *335*, 700−704.
(3) Frieden, C.; Hoeltzli, S. D.; Ropson, I. J. *Protein Sci.* **1993**, *2*, 2007−2014.
(4) Smith, D. L.; Deng, Y. Z.; Zhang, Z. Q. *J. Mass Spectrom.* **1997**, *32*, 135−146.
(5) Wang, F.; Li, W.; Emmett, M. R.; Hendrickson, C. L.; Marshall, A. G.; Zhang, Y. L.; Wu, L.; Zhang, Z. Y. *Biochemistry* **1998**, *37*, 15289−15299.
(6) Bowers, M. T.; Elleman, D. D. *J. Am. Chem. Soc.* **1970**, *92*, 1847.
(7) Inoue, M.; Wexler, S. *J. Am. Chem. Soc.* **1969**, *91*, 5730.
(8) Campbell, S.; Rodgers, M. T.; Marzluff, E. M.; Beauchamp, J. L. *J. Am. Chem. Soc.* **1995**, *117*, 12840−12854.
(9) Cheng, X. H.; Fenselau, C. *Int. J. Mass Spectrom. Ion Processes* **1992**, *122*, 109−119.
(10) Freitas, M. A.; Shi, S. D. H.; Hendrickson, C. L.; Marshall, A. G. *J. Am. Chem. Soc.* **1998**, *120*, 10187−10193.

(11) Freitas, M. A.; Marshall, A. G. *Int. J. Mass Spectrom.* **1999**, *183*, 221−231.
(12) Green, M. K.; Gard, E.; Bregar, J.; Lebrilla, C. B. *J. Mass Spectrom.* **1995**, *30*, 1103−1110.
(13) Smith, D. L.; Zhang, Z. Q. *Mass Spectrom. Rev.* **1994**, *13*, 411−429.
(14) Katta, V.; Chait, B. T. *Rapid Commun. Mass Spectrom.* **1991**, *5*, 214−217.
(15) Miranker, A.; Robinson, C. V.; Radford, S. E.; Aplin, R. T.; Dobson, C. M. *Science* **1993**, *262*, 896.
(16) Suckau, D.; Shi, Y.; Beu, S. C.; Senko, M. W.; Quinn, J. P.; Wampler, F. M.; McLafferty, F. W. *Proc. Natl. Acad. Sci. U.S.A.* **1993**, *90*, 790−793.
(17) Winger, B. E.; Lightwahl, K. J.; Rockwood, A. L.; Smith, R. D. *J. Am. Chem. Soc.* **1992**, *114*, 5897−5898.
(18) Freitas, M. A.; Hendrickson, C. L.; Emmett, M. R.; Marshall, A. G. *Int. J. Mass Spectrom.* **1999**, *187*, 565−575.
(19) Freitas, M. A.; Hendrickson, C. L.; Emmett, M. R.; Marshall, A. G. *J. Am. Soc. Mass Spectrom.* **1998**, *9*, 1012−1019.
(20) Bartmess, J. E.; McIver, R. T. In *Gas-Phase Ion Chemistry*; Bowers, M. T., Ed.; Academic Press: New York, 1979; Vol. 2, pp 88−121.
(21) Aue, D. H.; Bowers, M. T. In *Gas-Phase Ion Chemistry*; Bowers, M. T., Ed.; Academic Press: New York, 1979; Vol. 2, pp 1−51.
(22) Camara, E.; Green, M. K.; Penn, S. G.; Lebrilla, C. B. *J. Am. Chem. Soc.* **1996**, *118*, 8751−8752.
(23) Gong, S. N.; Camara, E.; He, F.; Green, M. K.; Lebrilla, C. B. *Int. J. Mass Spectrom.* **1999**, *187*, 401−412.
(24) Gard, E.; Green, M. K.; Bregar, J.; Lebrilla, C. B. *J. Am. Soc. Mass Spectrom.* **1994**, *5*, 623−631.
(25) Campbell, S.; Rodgers, M. T.; Marzluff, E. M.; Beauchamp, J. L. *J. Am. Chem. Soc.* **1994**, *116*, 9765−9766.
(26) Green, M. K.; Penn, S. G.; Lebrilla, C. B. *J. Am. Soc. Mass Spectrometry* **1995**, *12*, 1247−1251.
(27) Gard, E.; Willard, D.; Bregar, J.; Green, M. K.; Lebrilla, C. B. *Org. Mass Spectrom.* **1993**, *28*, 1632−1639.
(28) Wagner, D. S.; Melton, L. G.; Yan, Y.; Erickson, B. W.; Anderegg, R. J. *Protein Sci.* **1994**, *3*, 1305−1314.
(29) Zhang, Z. Q.; Li, W. Q.; Logan, T. M.; Li, M.; Marshall, A. G. *Protein Sci.* **1997**, *6*, 2203−2217.
(30) Green, M. K.; Lebrilla, C. B. *Mass Spectrom. Rev.* **1997**, *16*, 53−71.
(31) Ausloos, P.; Lias, S. G. *J. Am. Chem. Soc.* **1981**, *103*, 3641−3647.
(32) Hall, G.; Watt, J. M. *Modern Numerical Methods for Ordinary Differential Equations*; Clarendon Press: Oxford, 1976.
(33) Marshall, A. G.; Verdun, F. R. *Fourier Transforms in NMR, Optical, and Mass Spectrometry: A User's Handbook*; Elsevier: New York, 1990.
(34) Gill, P. E.; Murray, W. *National Physical Laboratory Report NAC* **1976**, *72*.
(35) Gill, P. E.; Murray, W. *J. Inst. Math. Appl.* **1972**, *9*, 91−108.
(36) Senko, M. W.; Hendrickson, C. L.; Pasatolic, L.; Marto, J. A.; White, F. M.; Guan, S. H.; Marshall, A. G. *Rapid Commun. Mass Spectrom.* **1996**, *10*, 1824−1828.
(37) Emmett, M. R.; Caprioli, R. M. *J. Am. Soc. Mass Spectrom.* **1994**, *5*, 605−613.
(38) Marshall, A. G.; Wang, T.-C. L.; Ticca, T. L. *J. Am. Chem. Soc.* **1985**, *107*, 7893−7897.
(39) Guan, S.; Marshall, A. G. *Int. J. Mass Spectrom. Ion Processes* **1996**, *157/158*, 5−37.